

## Coulomb blockade by electron-hole pairs in coupled single-electron transistors

Mincheol Shin,\* Seongjae Lee, and Kyoung Wan Park

*Electronics and Telecommunications Research Institute, Yusong P.O. Box 106, Taejeon 305-600, Republic of Korea*

Gwang-Hee Kim

*Department of Physics, Sejong University, Seoul 134-747, Republic of Korea*

(Received 21 April 2000)

We have theoretically investigated parallel coupled single-electron transistors (SET's) at strong coupling. We have found that the Coulomb diamond of the coupled SET's fragments into subdomains—triangular strips—which can be labeled by the number of electron-hole pairs and whose number increases as the coupling strengthens. The Coulomb blockading electron-hole pairs lead to the appearance of satellite Coulomb blockade oscillations in the expanded insulating region.

Recently, much attention has been given to series and parallel coupled metal and semiconducting systems which exhibit the Coulomb blockade (CB) effect. Numerous studies on the series coupled systems have focused on the role of the dot-to-dot coupling on the electronic and transport properties of the systems.<sup>1</sup> On the other hand, in most of the studies involving the parallel coupled systems, one of two parallel circuits served as an electrometer to detect the potential changes of the other device circuit, and for that purpose, weak coupling was considered.<sup>2-5</sup> There have been, however, a few interesting studies on the parallel coupled systems with strong coupling; the exciton transport in the Coulomb blockade regime was investigated theoretically<sup>6</sup> and experimentally<sup>7</sup> in strongly coupled parallel arrays, and the interaction between two pairs of double dots were investigated with both of the parallel arrays in the conducting state.<sup>8</sup>

The system we consider in this work is parallel coupled single-electron transistors at strong coupling. For weak coupling, the transport characteristics of the coupled SET's are the same as those of the single SET, with the stability diagram exhibiting usual Coulomb diamonds. When the coupling becomes sufficiently strong, however, electron-hole binding becomes important as in the case of the strong coupled arrays considered in Refs. 6 and 7, but in contrast to the previous works carried out in the cotunneling-dominating CB regime, we study *e-h* binding in the sequential-tunneling-dominating conducting regime and the dependence of the number of the *e-h* pairs on the charges induced by a side gate. The major findings in this work are that the Coulomb diamonds in the conducting regime break up into *fine internal structures* at strong coupling, and that, although the cotunneling processes are much less frequent, they nonetheless play a crucial role.

The coupled SET's comprise two metallic islands. To each island separate electrodes of source, drain, and gate are attached (see Fig. 1) and the two islands are capacitively coupled with capacitance  $C_\alpha$ . For simplicity, we assume that the four tunnel junctions in the system are identical with capacitances  $C$  and resistances  $R$ . Only the lower SET of the coupled SET's is active. Namely, we apply the symmetric bias voltage  $V$  and the gate voltage  $V_g$  to the lower SET, but ground all the electrodes of the upper SET. (The upper gate is omitted in the figure. In the following, we nevertheless

assume that it is attached to island 2, but inclusion of the upper gate is only *a matter of formality* to avoid unnecessary complications.)

At zero gate voltage, the potentials  $\phi_1$  and  $\phi_2$  of islands 1 and 2, respectively, are given by

$$\phi_1 = -\psi_0[n_1 + C_\alpha n_2 / (C_\alpha + 2)], \tag{1}$$

$$\phi_2 = -\psi_0[n_2 + C_\alpha n_1 / (C_\alpha + 2)], \tag{2}$$

where

$$\psi_0 = (C_\alpha + 2) / 4(C_\alpha + 1) \tag{3}$$

and  $n_1$  and  $n_2$  are the net charges on islands 1 and 2, respectively. Capacitance and potential were scaled by the units  $\tilde{C} = C + C_g/2$  and  $\tilde{V} = e/\tilde{C}$ , respectively. The electrostatic energy  $E(n_1, n_2)$  for a charge configuration  $(n_1, n_2)$  is then

$$E(n_1, n_2) = \psi_0(n_1^2 + n_2^2) / 2 + C_\alpha n_1 n_2 / 4(C_\alpha + 1). \tag{4}$$

To account for the lower gate at voltage  $V_g$ , we simply rewrite the above equations by replacing  $n_1$  with  $n_1 + Q_g$  where  $Q_g \equiv -C_g V_g$ .

The electrostatic energy is minimized when  $n_2 = -n_1 = n$ , that is, the system prefers to form the *e-h* pairs on islands 1 and 2. If we consider the sequential tunneling only (see below the effect of cotunneling), the mechanism for this pair formation is transfer of a charge to island 1, followed by attraction of a charge with opposite sign to island 2 by the Coulomb interaction. But if the charging energy for the addition of the charge on island 2 [the first term of Eq. (4)] is greater than the Coulomb-energy drop by the formation of a

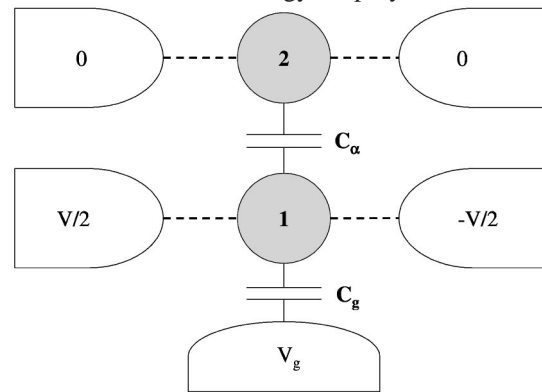


FIG. 1. Parallel coupled single-electron transistors. The dotted lines represent tunnel junctions.

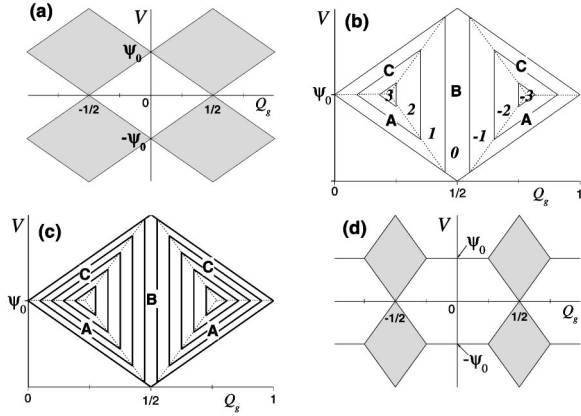


FIG. 2. In (a), the Coulomb diamonds for  $C_\alpha < 2$  are shown. The conducting diamonds that are fragmented at stronger couplings are shaded. (b) and (c) are the stability diagrams for  $C_\alpha = 20$  and 40, respectively. In (b), the strips with stable states  $(-n, n)$  are marked with the corresponding number  $n$ , and in (c), dotted lines delimit the three regions mentioned in the text. (d) is the stability diagram in the limit of strong coupling, where the reduced conducting diamonds are shaded.

$e$ - $h$  pair [the second term of Eq. (4)], it would not be attracted to island 2. Then, from the condition that  $\Delta E = E(-1, 1) - E(-1, 0) < 0$ , we obtain  $C_\alpha \geq 2$  for the  $e$ - $h$  formation. (Note that, since the upper SET is zero-biased,  $\Delta E = \Delta F$  for the addition of charges to island 2, where  $\Delta F$  is the free energy change.) In fact, for  $C_\alpha \leq 2$ , the upper SET insignificantly influences the lower SET and the stability diagram of the lower SET resembles that of a single SET [see Fig. 2(a)].

For strong coupling, or for  $C_\alpha \geq 2$ , electrons or holes are attracted to island 2 and, depending on the bias voltage  $V$  and the gate charge  $Q_g$ , they either are trapped there, or fluctuate with a certain mean value. When  $n$  charges are trapped on island 2, two possibilities arise in the lower SET: either  $-n$  charges are trapped on island 1, thereby producing  $e$ - $h$  pairs with  $n$  charges on island 2, or the tunneling processes  $-n \rightarrow -n-1 \rightarrow -n$  occur incessantly. Let us call the region where the former case holds region A and the latter region B. Specifically, in region A, the free energy  $F(-n, n) < F(-n \mp 1, n)$  and  $F(-n, n) < F(-n, n \pm 1)$  holds, so the charge configuration  $(-n, n)$  is a local minimum in the free energy space and thus *stationary*. Consequently, the lower SET is insulating in region A. In region B,  $F(-n, n) < F(-n, n \pm 1)$ , but  $F(-n, n) > F(-n-1, n)$  for tunneling over the left junction and  $F(-n-1, n) > F(-n, n)$  for tunneling over the right junction. Therefore the lower SET is conducting with the tunneling processes  $-n \rightarrow -n-1 \rightarrow -n$ . [But  $F(-n-1, n) < F(-n-1, n \pm 1)$  holds, so the  $n$  charges on island 2 remain trapped.]

As shown in Figs. 2(b) and 2(c), regions A and B occupy areas of the previously conducting diamonds [shaded diamonds in Fig. 2(a)]. The remaining regions of the previously conducting diamonds are denoted as region C in the figures. In region C, the charges on island 2 fluctuate with a certain mean value. Region C is comparable to region A: In region A, the charge configurations  $(-n, n)$  are stationary, but in region C, they fluctuate with  $(\langle n_1 \rangle, \langle n_2 \rangle) \approx (-n, n)$ .

If we index the areas of A, B, and C by  $n$  (in fact, by

$\langle n_2 \rangle \approx n$  for C), we obtain nested triangular structures as shown in Figs. 2(b) and 2(c).<sup>9</sup> There is an equal number of triangular strips in the left and right sides of the diamond separated by a medial vertical strip. For the left part, the outermost strip has  $n=1$ , and  $n$  increases by one as each strip is crossed inward. For the right part, we start with  $n=-1$  for the outermost strip, and  $n$  decreases one by one toward the innermost strip. The vertical strip at the center of the diamond corresponds to the state with  $n=0$ . See Fig. 2(b) where the strips are marked with corresponding  $n$ .

The boundaries of the nested triangular structures were drawn by the three sets of lines:

$$f_1(V, Q_g; n) = V - n/(C_\alpha + 1) - (1 - 2Q_g)\psi_0, \quad (5)$$

$$f_2(V, Q_g; n) = V + n/(C_\alpha + 1) - (1 + 2Q_g)\psi_0, \quad (6)$$

$$f_3(V, Q_g; n) = Q_g + 2n/C_\alpha - 1/2 - 1/C_\alpha, \quad (7)$$

which we obtain by considering the following six tunneling processes starting with the configuration  $(-n, n)$ . The free energy changes,  $\Delta F_{l,r}^\pm$ , for the single-electron tunneling processes over the left ( $l$ ) or right ( $r$ ) junction of the lower SET through which the number of electrons in island 1 changes by  $\pm 1$ , are given by

$$\Delta F_l^\pm = \mp (Q_g - 2n)\psi_0 + (\psi_0 \mp n \mp V)/2, \quad (8)$$

$$\Delta F_r^\pm = \mp (Q_g - 2n)\psi_0 + (\psi_0 \mp n \pm V)/2. \quad (9)$$

And the free energy changes  $\Delta f^\pm$  for the tunneling processes over the tunnel junctions of the upper SET are

$$\Delta f^\pm = \pm (Q_g - 2n)\psi_0 + (\psi_0 \mp Q_g \pm n)/2. \quad (10)$$

A remarkable feature in the stability diagrams at strong coupling is that the number of  $e$ - $h$  pairs constituting the stationary configurations strongly depends on the gate charge  $Q_g$ . At  $Q_g = 0$  and  $1/2$ , no  $e$ - $h$  pair can be formed, but at around  $Q_g = 1/4$  and  $3/4$ , the maximal number of  $e$ - $h$  pairs can be formed at  $V = \psi_0$ . Given  $C_\alpha$ , the maximal number of  $e$ - $h$  pairs or the number  $n_s$  of the triangular strips in each half of the fragmented conducting diamond is given by

$$n_s = [(C_\alpha + 2)^2 / 8(C_\alpha + 1)] \approx [C_\alpha / 8] \quad \text{for } C_\alpha \gg 1, \quad (11)$$

where  $[x]$  is the greatest integer not exceeding  $x$ . Therefore the conducting diamonds are more fragmented at stronger coupling, which is illustrated in Figs. 2(b) and 2(c). Only the conducting Coulomb diamonds [shaded ones in Fig. 2(a)] are divided into subdomains, while others remain intact.

One of the key results in this paper is the conversion of the previously conducting region to an insulating region (region A) by the formation of  $e$ - $h$  pairs. In the limit of very strong coupling, the insulating regions of the coupled SET's are thus expanded and take on a hexagonal shape, and as a consequence, the conducting diamonds are shrunk. See Fig. 2(d). Note that the conducting diamonds in the limit of  $C_\alpha \rightarrow \infty$  are shrunk by the ratio of  $1/4$  compared to those for  $C_\alpha = 0$ .

We have calculated the current  $I_1$  through the lower SET by solving the master equations<sup>10</sup> with cotunneling processes included, using the approximation by Jensen and Martinis.<sup>11</sup>

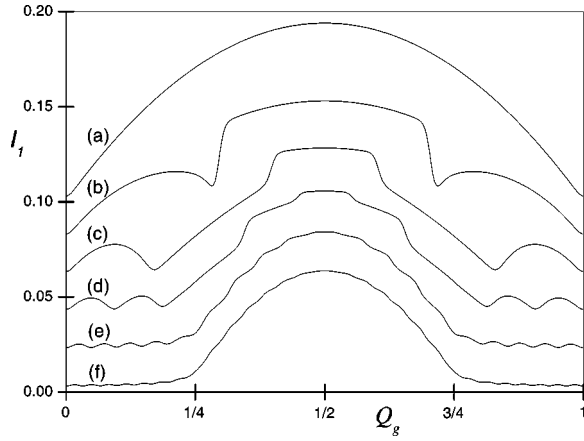


FIG. 3.  $Q_g$ - $I_1$  characteristics for  $C_\alpha=1(a), 5(b), 10(c), 20(d), 40(e)$ , and  $60(f)$ . For clearer view, each curve is offset by 0.02 from the one immediately below it. [The curve (f) has no offset.] The bias voltage  $V$  was fixed at  $\psi_0$ , and the resistance  $R=10^6 \Omega$  and  $T/\tilde{T}=0.001$ . The unit of current is  $e/R\tilde{C}$ .

Figure 3 shows the  $Q_g$ - $I_1$  characteristics for  $C_\alpha=1(a), 5(b), 10(c), 20(d), 40(e)$ , and  $60(f)$ . The bias voltages are fixed at  $V=\psi_0$  and temperature  $T/\tilde{T}=0.001$  where  $\tilde{T}=e^2/k_B\tilde{C}$ . First, note the gradual shrinkage of the conducting region as  $C_\alpha$  increases, from  $[0,1]$  for  $C_\alpha < 2$  to  $[1/4, 3/4]$  for  $C_\alpha \gg 1$ , which accords with the stability diagrams of Fig. 2. Second, as the key feature of the  $Q_g$ - $I_1$  characteristics, satellite oscillations are seen in the ‘tail’ regions of  $[0, 1/4]$  and  $[3/4, 1]$ , which correspond to region A of the stability diagram. The property of the oscillations is exactly the same as that of the CB oscillations of the usual SET. Namely, region A consists of multiple insulating phases labeled by the number of Coulomb-blocking  $e$ - $h$  pairs, and the oscillation peak arises during each transition from one insulating phase to another, whereby the number of  $e$ - $h$  pairs increases or decreases by one. Therefore, the number of oscillations, that equals to  $n_s$  of Eq. (11), increases as  $C_\alpha$  increases.

The  $e$ - $h$  CB oscillations are best seen at the bias voltage  $V$  close to  $\psi_0$ . Our numerical simulations indicated that if  $V \lesssim 3/4\psi_0$ , the oscillation amplitudes become so small compared to the background quantum fluctuations that the oscillations are hardly observed. Similar oscillations can also be seen in region C (by the similar argument applied for region A), although the oscillations are quickly blurred by the background currents as  $V$  is increased from  $\psi_0$ .

Third, in the central region ( $1/4 \leq Q_g \leq 3/4$ ) of Fig. 3, the currents show discrete jumps. Recall that in region B of the stability diagram to which the central region belongs,  $n$  charges are trapped on the upper island while the lower SET is conducting. From the viewpoint of the lower SET, the presence of  $n$  charges on the upper island is formally the same as if  $q_u$  charges were induced on the lower island by the upper island charges, where  $q_u(n) = C_\alpha n / (C_\alpha + 2)$ . Therefore, if  $n$  changes by 1, the effectively induced charge  $q_u$  changes discretely by  $C_\alpha / (C_\alpha + 2)$ , and so the current  $I_1$  jumps abruptly. See Fig. 4. Since  $n$  changes from  $n_s$  to  $-n_s$  in region B of the stability diagram, there exist  $2n_s$  such jumps for  $V = \psi_0$ . Clear jumps are observed in the entire area of region B of Figs. 2(b) and 2(c).

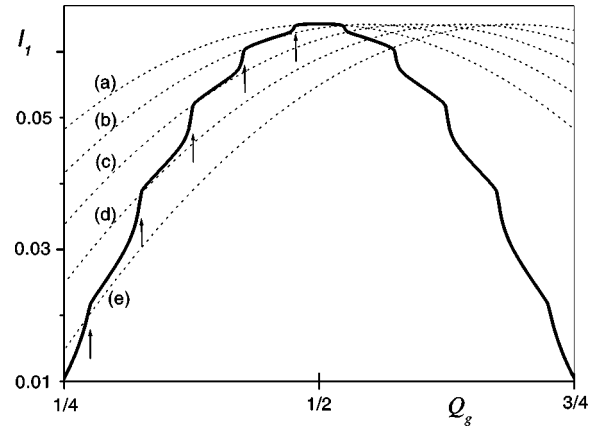


FIG. 4. Central region for  $C_\alpha=40$  at  $T=0$  (solid line). The dotted lines represent  $Q_g$ - $I_1$  curves of the equivalent SET with effectively induced charges  $q_u(n)$  on island 1 where  $n=0(a), 1(b), 2(c), 3(d)$ , and  $4(e)$ . The points where jump occurs are marked by arrows.

Our numerical simulations suggest that the above mentioned  $e$ - $h$  CB oscillations and current jumps are observed in the range accessible by experiments:  $R \geq 10^5 \Omega$ ,  $T \leq 10$  mK for  $\tilde{C} \sim 0.1$  fF and  $5 \leq C_\alpha/\tilde{C} \leq 50$ . And, although we applied symmetric biases to the lower SET and grounded the upper SET for convenience, we note that the physics should be the same independently of the detailed way of biasing the system, as long as the  $e$ - $h$  pairs can be formed as described in this work.

Let us now discuss the role of cotunneling in the hexagonal insulating region of the stability diagram. (In other regions, it simply acts as the usual background fluctuations.) The insulating region is represented by the configurations  $\mathbf{n}_0 \equiv (-n_0, n_0)$ , where

$$n_0 = [(C_\alpha + 1)V - (C_\alpha + 2)(1 - 2Q_g)/4] \quad (12)$$

if  $V \geq (1 - 2Q_g)\psi_0$ , and  $n_0 = 0$  otherwise. Recall that  $n_0$  is the stationary configuration satisfying  $F(-n_0, n_0) < F(-n_0 \mp 1, n_0)$  and  $F(-n_0, n_0) < F(-n_0, n_0 \pm 1)$ , and it is not necessarily the free-energy minimum. The relevant free-energy minimum is  $\mathbf{n}^+ = (-n^+, n^+)$ , where

$$n^+ = [(C_\alpha + 1)V/2 + Q_g/2], \quad (13)$$

which is obtained by minimizing the free energy  $F^+(-n, n) = E(-n, n) - nV/2$ . That  $n^+$  differs from  $n_0$  ( $n^+ \geq n_0$ ) implies the metastability of the configuration  $n_0$ . The fluctuations, which are caused by the thermally activated sequential tunneling or by the forward cotunneling that would bring the system from  $n_0$  toward  $n^+$ , would quickly move the system out of its local minimum  $n_0$  and settle it at the more stable point  $n^+$ , and the stability diagrams which were drawn based on  $\mathbf{n}_0$  would collapse. However, on the path between  $n_0$  and  $n^+$ , the backward cotunneling process [which promotes  $(-n, n) \rightarrow (-n+1, n-1)$ ] is dominant: its free energy change,

$$\Delta F_C^-(n, Q_g) = [(1 - Q_g)/2 + n]/(C_\alpha + 1) - V/2, \quad (14)$$

is much lower than  $\Delta F_C^+(n, Q_g) [= \Delta F_C^-(n, -Q_g)]$  of the forward cotunneling process, and its rate is much greater

than the thermally activated sequential tunneling rate at relatively low temperatures [ $\sim \exp(-\Delta F_S/k_B T)$ , where  $\Delta F_S (>0)$  is free-energy change of relevant sequential tunnelings]. Therefore, the backward cotunneling process prevents the system from drifting to  $n^+$  by pulling the system back to  $n_0$ . In short, by the combined effect of thermal and quantum fluctuations, the system fluctuates back and forth with  $n_0$  its midpoint. Our numerical simulations confirmed the restoration of the stability diagram by the quantum fluctuations at relatively low temperatures.

In conclusion, the Coulomb diamond of the coupled SET's at strong coupling fragments into subdomains which can be labeled by the number of  $e$ - $h$  pairs. As a consequence, the insulating regions considerably expand and take the shape of hexagons. In the expanded insulating region,

$e$ - $h$  pairs Coulomb-blockade the system, resulting in satellite Coulomb-blockade oscillations in a gate voltage sweep. In the shrunken conducting region, the current jumps are observed. In this paper, the coupling between SET's is purely capacitive, but the case where there is a resistor in parallel would be also interesting because the process of breakup and restoration of the  $e$ - $h$  pairs—which should be subject to the magnitude of the junction resistance—is expected to take place.

This work has been supported in part by the Ministry of Information and Communications of Korea, in part by KOSEF (Grant No. 1999-1-114-002-5) and in part by the NRL Program of Korea.

\*Email: mcshin@etri.re.kr

- <sup>1</sup>Among others, L.P. Kouwenhoven *et al.*, in *Proceedings of the Advanced Study Institute on Mesoscopic Electron Transport*, edited by L.L. Sohn, L.P. Kouwenhoven, and G. Schön (Kluwer, Dordrecht, 1997); D.G. Austing, T. Honda, K. Muraki, Y. Tokura, and S. Tarucha, *Physica B* **249**, 206 (1998); A. Georges and Y. Meir, *Phys. Rev. Lett.* **82**, 3508 (1999); R.H. Blick, R.J. Haug, J. Weis, D. Pfannkuche, K.v. Klitzing, and K. Eberl, *Phys. Rev. B* **53**, 7899 (1996).
- <sup>2</sup>V.A. Krupenin, S.V. Lotkhov, H. Scherer, Th. Weimann, A.B. Zorin, F.-J. Ahlers, J. Niemeyer, and H. Wolf, *Phys. Rev. B* **59**, 10 778 (1999).
- <sup>3</sup>I. Amlani, A.O. Orlov, G.L. Snider, C.S. Lent, and G.H. Bernstein, *Appl. Phys. Lett.* **71**, 1730 (1997).
- <sup>4</sup>L.W. Molenkamp, K. Flensberg, and M. Kemerink, *Phys. Rev. Lett.* **75**, 4282 (1995).

- <sup>5</sup>M. Koltonyuk, D. Berman, N.B. Zhitenev, R.C. Ashoori, L.N. Pfeiffer, and K.W. West, *Appl. Phys. Lett.* **74**, 555 (1999).
- <sup>6</sup>D.V. Averin, A.N. Korotkov, and Yu.V. Nazarov, *Phys. Rev. Lett.* **66**, 2818 (1991).
- <sup>7</sup>M. Matters, J.J. Versluys, and J.E. Mooij, *Phys. Rev. Lett.* **78**, 2469 (1997).
- <sup>8</sup>A.O. Orlov, I. Amlani, G. Toth, C.S. Lent, G.H. Bernstein, and G.L. Snider, *Appl. Phys. Lett.* **73**, 2787 (1998).
- <sup>9</sup>The stability diagrams are more complex in a closer examination: especially, region *C* is rather approximately drawn. The details are irrelevant in the discussions in this paper and will be published elsewhere.
- <sup>10</sup>M. Shin, S. Lee, K.W. Park, and E.-H. Lee, *Phys. Rev. B* **59**, 3160 (1999).
- <sup>11</sup>H.D. Jensen and J.M. Martinis, *Phys. Rev. B* **46**, 13 407 (1992).